

pubs.acs.org/journal/aidcbc Article

Indole Facilitates Antimicrobial Uptake in Bacteria

Tong Wu, Michael J. Wilhelm,* Yujie Li, Jianqiang Ma, and Hai-Lung Dai



Cite This: ACS Infect. Dis. 2022, 8, 1124-1133



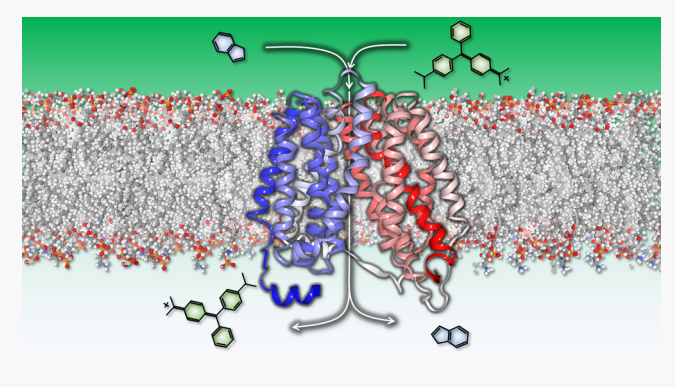
ACCESS

Metrics & More



Supporting Information

ABSTRACT: Indole signaling in bacteria plays an important role in antibiotic resistance, persistence, and tolerance. Here, we used the nonlinear optical technique, second-harmonic light scattering (SHS), to examine the influence of exogenous indole on the bacterial uptake of the antimicrobial quaternary ammonium cation (qac), malachite green. The transport rates of the antimicrobial qac across the individual membranes of *Escherichia coli* and *Pseudomonas aeruginosa*, as well as liposomes composed of the polar lipid extract of *E. coli*, were directly measured using timeresolved SHS. Whereas exogenous indole was shown to induce a 2-fold increase in the transport rate of the qac across the cytoplasmic membranes of the wild-type bacteria, it had no influence on a knockout strain of *E. coli* lacking the tryptophan-specific transport



protein (Δmtr). Likewise, indole did not affect the transport rate of the qac diffusing across the liposome membrane. Our findings suggest that indole increases the bacterial uptake of antimicrobials through an interaction with the Mtr permease.

KEYWORDS: persister cells, Mtr permease, membrane permeability, E. coli, P. aeruginosa, second-harmonic generation

Indole is a bacterial signaling molecule known to be produced by at least 85 different species of bacteria spanning both Gram-positive and Gram-negative strains. 1-3 It participates in both interspecies and interkingdom signaling and has been implicated in the regulation of bacterial persister formation, 5-10 biofilm formation, plasmid stability, 11 and antibiotic resistance and tolerance. 12,13 As an interkingdom signaling molecule, indole influences brain development and aging, 14 liver function, 14 mood, 15 tissue damage, 16 skin, 17 and Alzheimer's disease. 18

The influence of indole on the formation of bacterial persister cells has received considerable attention in recent years. 5–9,19 Bacterial persisters are a dormant subpopulation of an otherwise genetically identical group of cells but exhibit reduced metabolic activity and therefore have a tendency to better tolerate an antimicrobial challenge. Persister cells are often experimentally identified as the surviving population of cells following lethal application of a given physiologic stress (e.g., heat, pH, antibiotic). 21

Vega et al. reported that extracellular indole triggers a stress response and initiates the formation of persister cells. They showed that inoculation with physiological concentrations of indole to *Escherichia coli* (grown in tryptophan-free medium) significantly increased (i.e., by an order of magnitude) the percentage of cells surviving treatment with the antimicrobial, ofloxacin. They also found that indole did not induce persistence in mutant strains (Δmtr) lacking the tryptophan-specific importer, Mtr permease.

However, as noted in the reviews by Song and Zarkan, 19,22 several follow-up studies have since shown the exact opposite behavior that exogenous indole actually reduced persister formation. $^{5,7,8,23-25}$ In contrast to Vega et al.'s conclusions, 6 these more recent studies suggest that extracellular indole actually increases antibiotic efficacy. For example, Wood and co-workers showed that indole reduced persistence in tryptophanase knockout strains ($\Delta tnaA$) of $E.\ coli$ following treatment with either ampicillin or ciprofloxacin. 5,8 Overall, when Mtr permease is absent (as in the Δmtr -knockout strain), the influence of indole is reduced. Based upon these observations, it is reasonable to speculate that the effect of indole on antibiotic efficacy is driven by its interactions with bacteria membrane proteins.

The influence of indole on the physical properties of model membranes, such as liposomes, has previously been reported.^{26–29} For example, Eisenbach et al. employed fluorescence polarization measurements and saw no effect of indole on the microviscosity of liposome membranes, suggesting that indole does not induce a variation in membrane fluidity.²⁸ Likewise, Cama showed that the passive membrane permeability of a liposome in response to the

Received: November 23, 2021 Published: March 17, 2022





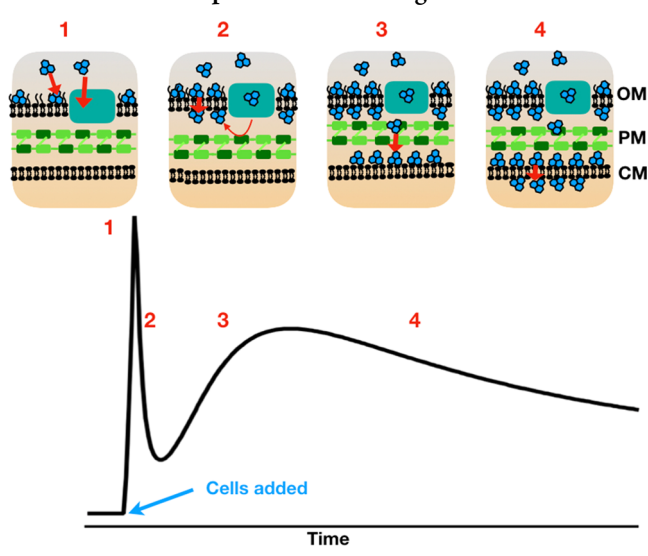
antibiotic norfloxacin was not significantly influenced by the presence of exogenous indole. These results highlight the absence of the influence of indole on liposomes lacking membrane-embedded proteins. These observations are consistent with the results from knockout strain studies and reinforce the speculation that the presence of the Mtr permease is necessary for indole to modulate antibiotic efficacy.

To gain a mechanistic understanding of the effect of indole on antibiotic efficacy, we examine how the presence of indole affects the relative permeability of antibiotics in bacterial membranes. Specifically, we examine the interaction of indole with the Gram-negative bacterial cell wall complex, which consists of dual protein-embedded phospholipid membranes separated by a thin layer of peptidoglycan. We report here observations quantifying the influence of indole on the permeability of individual membranes within this complex cell wall structure.

We have previously demonstrated the nonlinear optical technique, second-harmonic light scattering (SHS) as a means of measuring molecular transport rates across individual membranes in living bacteria. ^{30,31} We have also shown that this method can be used to quantitatively monitor chemically induced changes (including those brought about by antibiotics) in membrane permeability.³² Briefly, time-resolved SHS is based upon the physical phenomenon, secondharmonic generation (SHG), in which a molecule lacking inversion symmetry (i.e., noncentrosymmetric) is capable of producing second-harmonic (SH) light following irradiation with intense laser light. $^{33-35}$ The term SHS is used here for describing SHG from biological cells because the overall SH signal produced from micron size colloidal particles has an angular scattering pattern. $^{33-35}$ In describing SHS from the molecules at the membrane surface, we first point out that an ensemble of SHG-active molecules randomly oriented in liquid solution does not yield an SHG signal as the SH fields generated by these individual molecules cancel with each other.³³ However, as SHG-active molecules adsorb onto a surface (e.g., the exterior leaflet of a cell membrane), their molecular orientations become aligned due to the similarity of the molecule-surface interactions. Here, the SH fields generated by the aligned molecules constructively interfere with each other and produce a detectable time-dependent SH signal, which scales as the square of the surface density of the adsorbed molecules.³⁶ As the molecules transport across the membrane and adsorb onto the inner leaflet, their orientation is exactly opposite to those molecules adsorbed on the outer leaflet. Consequently, the SH fields generated by molecules on the opposite sides of the membrane cancel out and the resulting SH signal begins to decrease. 37,38 The rate of the signal decrease reflects how fast molecules are diffusing across the membrane. This is the general basis from which SHS can be used to monitor molecular transport across a membrane.

To illustrate how SHS can be used to monitor molecular interactions with living cells, Scheme 1 depicts the characteristic SHS signal response during the various stages of molecular transport across the dual phospholipid membranes of Gramnegative bacteria. Prior to the addition of bacteria cells into the sample, the randomly oriented ensemble of SHG-active molecules yields only an incoherent background response. However, once cells are added into the solution (panel 1), a coherent SHS signal rises due to saturated adsorption of the SHG-active molecules onto the outer leaflet of the outer

Scheme 1. Characteristic Time-Resolved SHS Response for an Ensemble of SHG-Active Molecules Transporting across the Cell Wall Complex of a Gram-Negative Bacterium



membrane (OM). As the SHG-active molecules cross the outer membrane protein (Omp) channels and begin to adsorb onto the interior leaflet of the OM (panel 2), the SHS signal starts to decay due to cancellation of the SHS signal generated from the SHG-active molecules adsorbed on the opposite sides of the membrane. Next, as the SHG-active molecules diffuse through the peptidoglycan mesh (PM) and arrive at and adsorb onto the exterior surface of the cytoplasmic membrane (CM), the SHS signal once again begins to rise, albeit at a comparatively slower rate due to diffusion-limited transport through the PM (panel 3). Finally, at later time, the SHS signal once again begins to decay as the SHG-active molecules gradually diffuse across the hydrophobic interior of the CM, enter the cytosol, and begin to adsorb onto the interior surface of the CM (panel 4). The signal decay here stems from cancellation of SHS due to the opposing orientations of the SHG-active molecules on the opposite sides of the CM. This interpretation of the time-dependent SHS response has been verified in numerous prior studies of liposomes, ^{39–42} living bacteria, ^{43–45} and validated using time-resolved brightfield transmission microscopy. ^{46,47}

By measuring the time-dependent response of the SHS signal following the addition of cells into the sample reservoir, the molecular transport rate at each individual interface within the complex wall can be deduced. 45,48,49 Consequently, any chemically induced changes to membrane permeability can be assessed by measuring the transport rates before and after a given physiological stress (e.g., addition of an antibiotic). We have previously used this approach to quantify the dose-dependent changes in the passive transport rate of the SHG-active molecular cation, malachite green (MG), across *E. coli* membranes in response to azithromycin 50 and adenosine triphosphate. 32

Herein, we employ time-resolved SHS to examine whether exogenous indole alters membrane permeability for antimicrobial compounds. Specifically, we examine the influence of indole on the passive uptake of cationic MG. In addition to being SHG-active, MG belongs to the family of quaternary ammonium cations (qac) (i.e., which comprise the active ingredients of the commercial disinfectant, Lysol) and is

known to exhibit antimicrobial effects. ⁵¹ We begin by running a series of control experiments without indole to determine the baseline MG transport rates for all of the bacterial strains under investigation. As representative examples, wild-type strains of $E.\ coli$ and $Pseudomonas\ aeruginosa$ were chosen for study. Additionally, we examine Δ mtr-knockout strains of $E.\ coli$, as well as biomimetic liposomes constructed from the polar lipid extract of $E.\ coli$. We then repeated our MG uptake measurements in the presence of indole. Any observed change in the deduced transport rates can be attributed to the influence of indole on the membrane. The influence of indole as a membrane permeabilizer and the role of the Mtr permease in increasing antibiotic efficacy will be discussed.

RESULTS

Extracellular Indole Increases the Permeability of the Cytoplasmic Membrane in Wild-Type E. coli and P. aeruginosa. We first examine the influence of extracellular indole on the permeability of bacterial membranes by measuring the transport rates of the MG cation through the individual membranes of wild-type E. coli and P. aeruginosa.

Figure 1 depicts representative time-resolved SHS signals corresponding to the bacterial uptake of MG in the absence

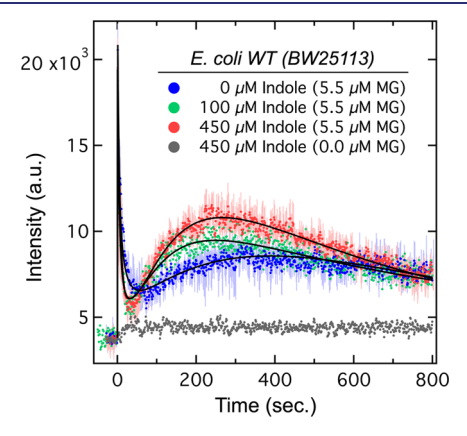


Figure 1. Time-resolved SHS response from MG cations (0 or 5.5 μ M) interacting with *E. coli* (*BW25113*) in the absence (blue points) or presence (red and green points) of indole. The gray points highlight the weak static SHS signal arising from indole interacting with the bacteria without MG. Lighter color vertical lines represent the uncertainty of each point deduced as the standard deviation from a minimum of three runs. Solid black lines represent a nonlinear least-squares fit based on the kinetic model.

(blue points) and presence of extracellular indole (red points: 450 μ M indole; green points: 100 μ M indole). The high concentration of indole examined here was chosen to mimic the experimental conditions employed in the initial studies examining the influence of indole on persister formation. 5,6,8 The SHS signal measured here originates almost exclusively from cationic MG at the various surfaces within the bacterial wall structure (Figure 1). Given that indole is noncentrosymmetric, it may have a nonzero hyperpolarizability and may be able to produce coherent SHS. However, under the conditions of our experiment, indole produces only a weak, nonresonance enhanced SHS response as shown by the gray points in Figure 1, where a nominal static increase in the baseline signal intensity is observed for our control experiment consisting of 450 μ M indole without MG. This static contribution is removed from the data prior to fit analysis. Furthermore, we

note here that, even though MG is an antimicrobial compound, ⁵¹ the employed concentration of 5.5 μ M is well below the deduced minimum inhibitory concentration (MIC) value of 100 μ M for our wild-type strain of *E. coli*. ⁵⁰ Further, UV–vis spectra revealed that MG does not react with indole (see the Supporting Information, SI for additional details). Consequently, the difference in the SHS signals arising from MG cations adsorbed on the bacterial membranes (with or without indole) solely reflects the influence of indole-induced changes in membrane properties.

The kinetic traces depicted in Figure 1 are qualitatively similar and consist of an initial rapid transport event (i.e., rise and decay of the SHS signal) followed by a considerably slower secondary transport event. The initial transport events are effectively identical in terms of the magnitude and the time response. The similarity of the signal magnitudes (which scales as the density of MG on the membrane surface), observed with and without indole, suggests that indole does not compete against MG ions for surface adsorption sites. This is reasonable given that adsorption of cationic MG onto membrane surfaces is primarily driven by electrostatic attraction and indole is a charge neutral molecule.

The time responses of the initial transport events can be characterized as an instantaneous rise of the signal followed by a decay over a duration of roughly 40 s. As depicted in Scheme 1, this corresponds to the efficient transport of MG across the bacterial OM through the Omp channels. Beyond the first peak, the two signals (with and without indole) begin to show distinctly different kinetic behavior. Specifically, the presence of extracellular indole results in a noticeably faster secondary rise of the signal (peaking around 250 s) as well as a faster secondary decay of the signal. The faster rise suggests that in the presence of indole, MG cations are able to traverse the bacterial PM at a faster rate and arrive at the outer leaflet of the CM sooner. The faster decay indicates that indole enhances the passive diffusion of MG across the bacterial CM.

The influence of extracellular indole on the uptake of MG by *P. aeruginosa* is shown in Figure 2. Unlike *E. coli, P. aeruginosa* does not synthesize indole but instead scavenges it from its local environment. S2,53 Similar to the observations for *E. coli* (Figure 1), *P. aeruginosa* also exhibits an indole-induced

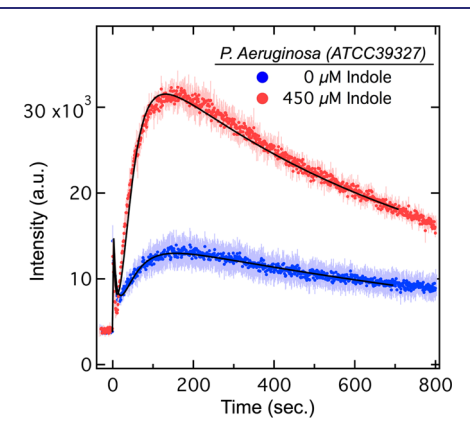


Figure 2. Time-resolved SHS responses for MG ions (5.5 μ M) interacting with *P. aeruginosa* (*ATCC39327*) in the presence (red circles) and absence (blue circles) of indole. Lighter color vertical lines represent the uncertainty of each point deduced as the standard deviation from a minimum of three runs. Solid black lines represent a nonlinear least-squares fit based on the kinetic model.

Table 1. Fit-Deduced Transport Rates for MG Cations Crossing the OM, PM, and CM of E. coli (BW25113), P. aeruginosa (ATCC39327) and E. coli (JW3130-1), with or without the Treatment of Indole^a

strains	$[Indole]/\mu M$	$k_{\rm Omp}\times 10^{-2}~{\rm s}^{-1}$	$k_{\rm PM} \times 10^{-2} \ {\rm s}^{-1}$	$k_{\rm CM} \times 10^{-4} \; {\rm s}^{-1}$
E. coli WT BW25113	0	1.14 ± 0.16	1.43 ± 0.15	5.10 ± 0.10
	100	1.14 ± 0.12	2.05 ± 0.08	8.30 ± 0.12
	450	1.24 ± 0.15	2.68 ± 0.19	9.89 ± 0.15
P. aeruginosa ATCC39327	0	2.40 ± 0.40	1.12 ± 0.11	6.47 ± 0.13
	450	2.08 ± 0.30	2.36 ± 0.14	10.60 ± 0.25
E. coli Δmtr JW3130-1	0	1.10 ± 0.11	1.12 ± 0.11	5.36 ± 0.26
	450	1.15 ± 0.09	2.36 ± 0.14	4.99 ± 0.28

^aError bars were deduced by averaging across minimally three repeated trials.

enhancement in the passive diffusion rate for MG crossing the bacterial PM and CM. It is also worth noting that the SHS intensity pattern for *E. coli* and *P. aeruginosa* are qualitatively different. Specifically, whereas the OM transport peak is stronger than the CM transport peak for *E. coli* (Figure 1), the opposite is observed for *P. aeruginosa* (Figure 2). The SHS intensity scales as the square of the molecular density adsorbed to the surface. The observed variations in SHS intensity simply indicate different concentrations of MG adsorbed on the various membrane surfaces, which reflects variations in membrane composition across different bacterial strains.

Quantitative analysis using our previously developed kinetic model of molecular transport permits determination of transport rates at various bacterial interfaces, including the OM, the PM, and the CM. Briefly, the measured SHS signal can be modeled as the square of the sum of the differences of the MG densities on each leaflet of the two bacterial membranes

$$I_{\text{SHS}}(t)$$

$$\sim [\{N_{\text{out}}^{\text{OM}}(t) - N_{\text{in}}^{\text{OM}}(t)\} + \{N_{\text{out}}^{\text{CM}}(t) - N_{\text{in}}^{\text{CM}}(t)\}]^2$$
(1)

where $N_{\text{out}}^{\text{OM}}(t)$, $N_{\text{in}}^{\text{CM}}(t)$, $N_{\text{out}}^{\text{CM}}(t)$, and $N_{\text{in}}^{\text{CM}}(t)$ are the timedependent molecular surface densities of cationic MG on the outer and inner leaflets of the OM and the outer and inner leaflets of the CM, respectively. The time dependence of these surface densities are largely dictated by the MG ion concentrations in the solution and in the various compartments within the cell, as well as the MG transport rates across the OM, the PM, and the CM. A coupled series of differential equations can be defined for modeling the time dependence of these concentrations and surface densities (see the SI for additional details). A nonlinear least-squares fitting of the observed time-dependent SHS signal, based upon the above model, can then be used to deduce the molecular transport rate for each interface. For each set of experimental conditions, there were minimally three repeated trials. In our fit analysis, each trace was individually fit to our kinetic model. All fit parameters (see the SI for additional details) were allowed to vary freely. The associated error for each fit parameter was deduced by averaging across repeated trials.

As tabulated in Table 1, for both *E. coli* and *P. aeruginosa*, the presence of extracellular indole results in a more than 2-fold increase in the MG transport rates across the bacterial PM and CM. The magnitude of the increased transport rates appears to scale with indole concentration. Conversely, transport across the bacterial Omp channels in the OM appears to be completely unaffected by indole. These results quantitatively demonstrate that extracellular indole does not influence

transport across the Omp channels but enhances passive diffusion across the PM and the CM.

Indole-Induced Membrane Permeability Changes in Liposomes and *mtr*-Knockout Strains of *E. coli*. In an effort to isolate the indole-specific interaction that is responsible for its influence on membrane transport, we ran a series of SHS experiments using liposomes as well as *mtr*-knockout strains of *E. coli*.

Indole Has No Influence on Passive Diffusion across Phospholipid Bilayers. Liposomes constructed from the polar lipid extract of *E. coli* are reasonable biomimetic surrogates of the bacterial CM, with the main exception being that they do not possess any protein. By repeating the SHS experiments with these liposomes, we can test whether the observed indole-induced enhancement of membrane permeability stems from an interaction with the various phospholipids in the membrane. Figure 3 depicts the transport

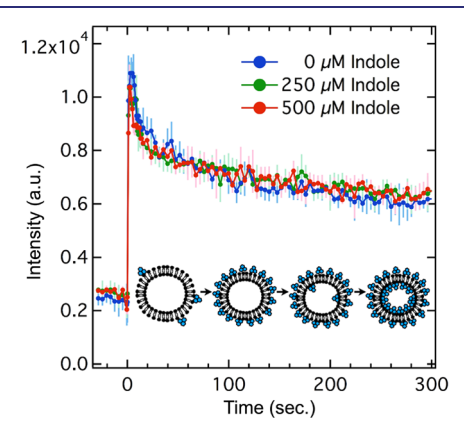


Figure 3. Time-resolved SHS responses for MG ions (5.5 μ M) interacting with the phospholipid membrane of a liposome in the presence (red and green circles) and absence (blue circles) of indole. Lighter color vertical lines represent the uncertainty of each point deduced as the standard deviation from a minimum of three runs. The cartoons below the traces mimic the adsorption and transport at the liposome membrane.

kinetics for MG crossing the liposome membrane in the presence and absence of indole. Unlike bacteria, the liposomes only possess a single membrane and hence give rise to only a single transport event. Nevertheless, regardless of the concentration of indole added, the time-resolved SHS signals were effectively identical, both in terms of their magnitude and kinetics.

Similar to the bacterial results (Figures 1 and 2), the invariance of the signal magnitude again suggests that there is no competition for adsorption sites between MG and indole.

Further, the invariance of the signal kinetics (signal decay rate) implies that MG is diffusing across the membrane with identical rates. The results of the fit analysis of the liposome experiments have been tabulated in Table 2. Within error, the

Table 2. Fit-Deduced Transport Rates for MG Cations Crossing the Phospholipid Bilayer of a Liposome Constructed from the Polar Lipid Extract of *E. coli* ^a

[Indole]	$0~\mu\mathrm{M}$	$250~\mu\mathrm{M}$	$500~\mu\mathrm{M}$
$k_{\rm mem} \times 10^{-3} \ {\rm s}^{-1}$	6.25 ± 0.15	6.72 ± 0.68	6.03 ± 0.27

[&]quot;Error bars were deduced by averaging across minimally three repeated trials.

MG transport rate for crossing the liposome membrane was shown to be completely independent of the presence of indole. Consequently, it becomes clear that the addition of extracellular indole does not influence the passive diffusion of MG across a pure (i.e., protein-free) phospholipid membrane. This suggests that the observed indole-induced enhancement of membrane permeability in bacteria likely stems from a protein-mediated process.

Indole Requires Mtr Permease to Increase Membrane Permeability. Prior studies have shown that bacteria lacking the Mtr permease showed a greater propensity to survive an antibiotic challenge. It is therefore reasonable to ask whether indole's observed influence on antibiotic resistance has any relation to this tryptophan transport protein. To assess whether or not Mtr is involved in the observed enhancement of MG transport, we repeated the SHS experiments using mtr-knockout strains of $E.\ coli.$ It should also be noted that, as there was no tryptophan in the sample media, additional indole was not produced by TnaA in the cytosol. 54

Figure 4 depicts the uptake of MG, in the presence or absence of indole, by the JW3130-1 knockout strain of *E. coli*. The initial transport peaks (i.e., for MG crossing the bacteria OM) are effectively the same as those observed in the wild-type strains of *E. coli* and *P. aeruginosa* (Figures 1 and 2). This is reasonable given that the Mtr permease is located in the CM; hence, the OM transport response should be similar to

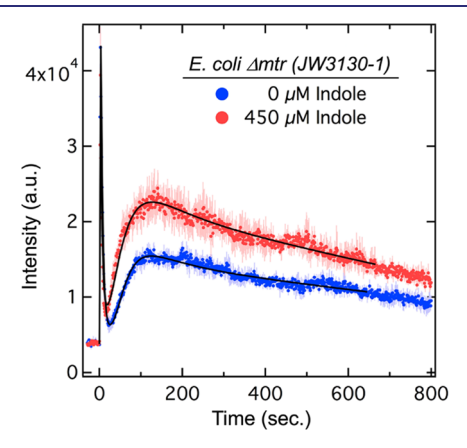


Figure 4. Time-resolved SHS responses for MG ions (5.5 μ M) interacting with the *mtr*-knockout strain of *E. coli (JW3130-1)*, in the presence (red circles) and absence (blue circles) of indole. Lighter color vertical lines represent the uncertainty of each point deduced as the standard deviation from a minimum of three runs. Solid black lines represent a nonlinear least-squares fit based on the kinetic model.

that observed in wild-type strains (Figure 1). For transport across the CM of the *mtr*-knockout strain, the presence of indole yields an overall increase in the magnitude of the signal. This is preceded by an apparent increase in the slope of the signal rise. Consistent with the wild-type sample, this is qualitatively suggestive of an increased transport rate across the PM (which was also observed in the wild-type strain). The most significant change, however, is the apparent invariance of the signal decay for the CM transport event. Unlike the wild-type sample (Figure 1), the decays of the second transport event are effectively parallel and therefore suggest that MG is transporting across the CM at the same rate. This observation suggests that, in the absence of the Mtr permease, the indole-induced enhancement of membrane permeability is turned off.

As above, the membrane transport rates for MG interacting with the *mtr*-knockout strain were determined from the measured SHS signals using our kinetic model of molecular transport (see the SI for additional details) and have been tabulated in Table 1. Consistent with the wild-type strain of *E. coli*, we observe that OM transport is independent of indole. Likewise, the deduced PM transport rate is still increased by more than half, which is reasonable given that the PM enhancement should be independent of the relative presence of the Mtr permease. Conversely, without the Mtr permease, the CM transport rate is no longer influenced by the presence of indole. This strongly suggests that the previously observed indole-induced enhancement of membrane permeability stems from an interaction involving indole and the Mtr permease.

DISCUSSION

Using time-resolved SHS, we were able to quantify the influence of exogenous indole in modulating the transport of an antimicrobial cation across membranes in living bacteria. In addition to increasing the rate of passive diffusion across peptidoglycan, it is observed that indole induces an increase in the permeability of the cytoplasmic membrane, but only when the Mtr permease is present. We now discuss the likely mechanism driving this indole-induced effect, using the results from the various experiments conducted. Following this, we will explore the potential for an indole-induced enhancement of membrane permeability as a means of improving the efficacy of antimicrobials that specifically target components within the bacterial cytosol.

Mechanism of Indole-Induced Enhancement of Membrane Permeability. Table 1 shows that regardless of whether indole was present in the sample, the transport rates for crossing the bacterial OM are invariant (within error). This was observed for *P. aeruginosa* as well as both strains of *E. coli*. This comparison, however, does not necessarily imply that transport across the OM was not influenced by the presence of indole. It is feasible that the influence of indole on transport across the OM is simply too small to be discerned. Specifically, the most efficient route for low-molecular-weight ions (ca. 650 g/mol or less) to cross the bacterial OM is through the various Omp channels, which perforate the OM. Nevertheless, as demonstrated in numerous prior studies, MG is capable of directly diffusing across the hydrophobic interior of a membrane. 37,55,56 The diffusion rate, however, is smaller than the Omp transport rate by 2 orders of magnitude. As shown in Table 1, whereas MG crosses the Omp channels at a rate of 10⁻² s⁻¹, it diffuses across the cytoplasmic membrane lipid bilayer at a staggeringly slower rate of 10⁻⁴ s⁻¹. On average, indole was shown to increase the transport rate across the CM

by a factor of 2. Consequently, even if indole doubled the rate for which MG passively diffused across the hydrophobic interior of the OM, this contribution is still orders of magnitude slower compared to that of the Omp channels. With all transport routes taken into account, the observed rate for MG crossing the OM should be primarily dictated by the Omp channels (i.e., the influence of indole on the permeability of the bacterial OM is undiscernible).

As compared to the OM, transport across the bacterial CM (i.e., which lacks passive transport channels) is restricted to passive diffusion across the hydrophobic interior. As noted in Table 1, for wild-type *E. coli*, this diffusion occurs with a rate of $5.1 \times 10^{-4} \, \rm s^{-1}$. However, in the presence of indole, this rate is shown to increase in a concentration-dependent manner: $8.3 \times 10^{-4} \, \rm s^{-1}$ (63% increase) for 100 μ M indole and $9.9 \times 10^{-4} \, \rm s^{-1}$ (94% increase) for 450 μ M indole. This observation seems to suggest that indole somehow enhances passive diffusion across the membrane. The biomimetic liposome results, on the other hand, do not support this interpretation.

Due to the fact that the liposome membrane purposely lacks proteins and various macromolecules (e.g., hopanoids), our liposome results allow us to focus on the effect of indole on the phospholipid membrane. As shown in Figure 3 and quantified in Table 1, regardless of the concentration of indole added, MG was shown to directly diffuse across the liposome membrane at a constant rate of ca. 6×10^{-3} s⁻¹. It is of interest to note that the deduced transport rate for passive diffusion across the liposome membrane is an order of magnitude faster compared to the bacterial CM (ca. 8 x 10^{-4} s⁻¹). This primarily stems from the fact that the liposome membrane lacks rigidifying compounds (e.g., hopanoids) and is therefore more fluid than the bacterial membrane. Significantly, the invariance of the passive diffusion rates as a function of indole concentration strongly suggests that the observed influence of indole is not modulation of passive diffusion across the lipid bilayer (e.g., disruption of phospholipid packing). This observation further suggests that indole is likely not influencing the permeability of the OM.

We now consider the observations based on the *mtr*-knockout strains of *E. coli*. Specifically, when the Mtr permease is absent from the bacterial CM, the influence of indole on transport across the CM disappears altogether (Figure 4 and Table 1). This observation is consistent with the notion that the effect of indole is not related to diffusive transport across the hydrophobic interior of the phospholipid membrane. Taking all of our observations into account, it becomes clear that the indole-induced enhancement of membrane permeability necessarily stems from an interaction with the Mtr permease.

So how then does the combination of indole and the Mtr permease result in more efficient MG transport across the bacterial CM? It is important to recall that the Mtr permease actively shuttles indole (and tryptophan) across the CM. Therefore, the most reasonable interpretation is that MG is somehow able to stowaway across the Mtr permease following initial activation by indole. For instance, the proposed topological model of the Mtr permease consists of $11~\alpha$ -helical transmembrane spans. One comparable and well-studied permease, the lactose permease, consists of $12~\alpha$ -helices and has a similar structure to Mtr. Based upon the current best model, lactose first specifically binds to a cluster of helices within the permease. This interaction results in a conformational change in which the tilt angle of the helices is

altered, which then releases the lactose into the cytosol. 59 We speculate that Mtr invokes a similar transport mechanism for indole. Presumably, MG alone is unable to bind to the helices in Mtr and is therefore unable to activate this channel by itself. However, during the indole-induced conformational change of the Mtr helices, it is feasible that MG passes through the Mtr along with indole. Such a mechanism is consistent with the fact that the increase in the transport rate across the CM scales with the concentration of indole. Specifically, as tabulated in Table 1, 100 μ M indole induces a 63% increase in the transport rate while 450 μM induces a 94% increase. In the presence of higher concentrations of indole, more Mtr channels can be activated, and hence, there are more routes for MG to stowaway across the CM. Although we currently have no direct experimental evidence to validate our stowaway hypothesis, such a mechanism could reasonably account for all of our observations. Nevertheless, additional experiments will be necessary to definitively prove such a mechanism.

Finally, we note that in addition to the observed indoleinduced (Mtr-assisted) enhancement of permeability across the bacterial CM, there is a concomitant enhancement in the diffusion rate through the peptidoglycan. This effect was observed for both P. aeruginosa and E. coli. As shown in Table 1, the rate of MG diffusion across the peptidoglycan is shown to increase with the concentration of indole. So how can we account for this indole-induced enhancement in the MG diffusion rate? Recall that peptidoglycans consist of glycan strands containing disaccharide units that are linked between carboxyl and amino groups.⁶⁰ For example, the carboxyl groups of chitin, which share a similar structure to peptidoglycan, can readily absorb cationic MG from aqueous solutions due to a favorable electrostatic interaction. ^{61,62} Ultimately, this transient adsorption hinders passive diffusion of cationic MG across the periplasm. While indole is a neutral molecule, it is highly polar^{63,64} and can therefore interact with polar portions of the peptidoglycan, including the disaccharide units, carboxyl groups, and carbonyl groups, via electrostatic and hydrogenbonding interactions. 65,66 Consequently, it is feasible that the adsorption of indole on the peptidoglycan should reduce the propensity for cationic MG adsorption and hence result in faster MG diffusion through the PM.

As indole competes against cationic MG to bind to the various anionic sites within the PM, this process should exhibit a concentration dependence. With more indole present, there are fewer anionic sites for MG cations to bind, and hence, MG cations would diffuse faster through the PM layer. Indeed, this is what was observed when we increased the concentration of indole from 100 to 450 μ M. As depicted in Figure 1 and quantified in Table 1, the presence of exogenous indole (whether 100 or 450 μ M) clearly increases the rate of diffusion across the PM. Specifically, 100 μ M indole induces a ca. 43% increase in diffusion rate, while 450 μ M indole increases the rate by ca. 87%.

Indole as a Means of Improving Antimicrobial Efficacy. Bacterial membranes protect cells from their local environment. In general, they prevent harmful chemicals from entering the cell and useful chemicals from leaving. Therefore, a popular antibiotic strategy is to attack bacterial membranes. Indeed, the modes of action of numerous antimicrobials include targeting membrane components, specific enzymes, and even DNA to alter membrane properties (e.g., fluidity, curvature, etc.), thereby weakening the protective function of the membrane. For example, aminoglycosides are known

to affect membrane composition by inserting mistranslated protein into the cytoplasmic membrane, thereby increasing membrane permeability and allowing increased access of antibiotics. ⁶⁹

In contrast to the work of Vega and co-workers,6 more recent studies have suggested that exogenous indole actually reduces the propensity for bacterial persistence.^{5,8} In these studies, persistence is measured by the size of the population, which survives (or persists) an antimicrobial challenge. In light of our observations that exogenous indole increases the diffusive transport rate of antimicrobials (i.e., MG) across the CM, it is reasonable to speculate that the influence of indole regarding persistence stems from indole's ability to improve the efficacy of antimicrobial compounds by enhancing their propensity to diffuse across the bacterial CM. For example, the specific antibiotics examined in prior indole-based persistence studies were known to induced bacterial cell death primarily by attacking targets located in the cytosol.^{68,70} To reach these targets, the antibiotics first had to successfully cross the cytoplasmic membrane and then achieve and maintain the requisite lethal concentration. Of importance, such a mechanism is limited by two opposing processes: (1) the rate at which the antimicrobial is able to cross the cytoplasmic membrane into the cytosol and (2) the counter influence of efflux pumps that work to expel such compounds.⁷¹ Therefore, the overall efficacy of these sorts of antimicrobials (i.e., whose biochemical targets are located within the cytosol) stems in part from the competition of the rate at which they can diffuse across the cytoplasmic membrane vs the rate at which they are effluxed out of the cell. Consequently, increasing the rate of uptake across the cytoplasmic membrane should result in a net increase of antimicrobial efficacy, which could initially be interpreted as a reduction in persistence.

It has previously been reported that cell viability in response to an antimicrobial attack significantly decreases in the presence of exogenous indole. 5,8 This behavior is consistent with our observations that the combination of exogenous indole and functional Mtr permease significantly increased the uptake rate of an antimicrobial cation into the cytosol. As discussed above, increasing the rate of influx of an antibiotic compound into the cytosol should result in an increase in antimicrobial efficacy. This understanding can also potentially explain why exogenous indole has been reported to reduce the propensity for bacterial persistence.^{5,8} Likewise, our results also provide a plausible explanation for the observation of higher survival rates for mtr-knockout strains under the same indole treatment.^{6,8} As both indole and functional Mtr are necessary to elicit an enhanced uptake of antimicrobial compounds, the absence of either component should result in standard uptake rates and hence a greater propensity to survive an antimicrobial

In summary, time-resolved second-harmonic light scattering was used to monitor indole-induced changes in membrane permeability for the antimicrobial quaternary ammonium cation, malachite green, in the membranes of *P. aeruginosa* and wild-type and *mtr*-knockout strains of *E. coli*. Membrane permeability was also quantified in biomimetic unilamellar liposomes constructed from the polar lipid extract of *E. coli*. For the wild-type strains of *P. aeruginosa* and *E. coli*, the transport rate for the antimicrobial cation crossing the bacterial CM was shown to double in the presence of indole. Conversely, for the *mtr*-knockout strain of *E. coli* and the liposome samples, no such indole-induced enhancement of

membrane permeability was observed. When considered together, these observations suggest that the observed indole-induced enhancement of transport across the bacteria CM is mediated through an interaction with the Mtr permease. It was suggested that indole-induced activation of the Mtr permease may permit simultaneous transport of MG across the channel. Nevertheless, the exact mechanistic details of the indole—Mtr permease interaction will require additional study. It was also observed that the presence of indole likewise enhances diffusion through the bacterial peptidoglycan mesh. It was reasoned that, as indole is highly polar, ⁶³ it can electrostatically adsorb to anionic sites within the peptidoglycan, hence preventing transient adsorption of the MG cation, thereby promoting faster diffusion of cations through the peptidoglycan.

MATERIALS

Bacteria Strains and Solutions. All bacteria samples were grown to the late-log/early stationary phase. Variations in the working cell density (OD_{600}) of the various bacterial strains were chosen to optimize the signal-to-noise ratio of the associated SHS experiments.

E. coli strains: K-12 BW25113 and JW3130-1 from the Keio collection collection collection collection collection collection CI were cultured at 37 °C (150 RPM shaking) in LB broth (Sigma-Aldrich) to an OD₆₀₀ \sim 1.5. To remove waste and residual growth medium, *E. coli* suspensions were centrifuged (1200g for 5 min) and resuspended with calcium and magnesium free 1 × phosphate-buffered saline, PBS(–) (Sigma-Aldrich). This process was repeated three times. The final *E. coli* stock solutions were diluted to an OD₆₀₀ \sim 2.5 with 1 × PBS(–). The residual baseline concentration of extracellular indole, following washing with PBS, was determined to be 5.86 μM as measured using Kovács Reagent (additional details in the Supporting Information, SI). Due to the absence of tryptophan in the supernatant, no additional indole can be produced by the cells in the stock solution.

P. aeruginosa (ATCC39327) was cultured at 26 °C (200 RPM shaking) in BD nutrition broth (Fisher Scientific) for 16 h to an $\mathrm{OD}_{600} \sim 1.8$. The cells were then washed in 1 × PBS(-) using the same protocol outlined above. The final *P. aeruginosa* stock solutions were diluted to an $\mathrm{OD}_{600} \sim 0.6$ with 1 × PBS(-).

Indole, malachite green oxalate salt, Kovács reagent, and dimethyl sulfoxide (DMSO) were purchased from Millipore Sigma. Due to limited solubility, indole was first dissolved in DMSO and then diluted with distilled water. The final concentration of DMSO in all experiments was 1% by volume. This concentration of DMSO was specifically chosen as it was sufficiently high to render indole soluble in water but not high enough to hinder bacterial viability (see the SI for additional details).

Liposome Preparation. The polar lipid extract of *E. coli*, consisting of 67% phosphatidyl ethanolamine (PE), 23.2% phosphatidyl glycerol (PG), and 9.8% cardiolipin (CL), was obtained from Avanti Polar Lipid Inc. As the lipid sample was isolated from a biological source, the composition of acyl chains invariably consist of a broad distribution of chain lengths and degree of unsaturation. This information was not provided by the distributor (Avanti Polar Lipid Inc.), and no attempt was made to characterize it further. Monodisperse unilamellar liposomes were prepared using the extrusion method.⁷⁵ All liposomes were prepared in 1 × PBS(–). Dynamic light scattering was used to determine the average

diameter of the liposomes, which was deduced to be 120 \pm 22 nm. The working density of liposome particles was ca. 9 \times 10 12 mL $^{-1}$.

Time-Resolved Second-Harmonic Light Scattering. A liquid jet was formed from a reservoir containing the colloidal sample (bacteria or liposomes) to interact with the laser beam for the SHS measurements. The setup for our SHS and liquid flow system has been described in detail previously. 50 Briefly, a Ti:Sapphire laser (Coherent, Micra V., oscillator only, 150 fs FWHM pulse duration,76 MHz repetition rate, 0.3 mW average output power, and 4 nJ pulse energy) was employed as the fundamental light source at 820 nm. The sample in the reservoir, containing bacteria or liposomes, was continuously circulated through a liquid flow jet pump (Micropump, Inc.). The laser beam was focused into the center of the liquid jet with a Rayleigh length of 1.6 mm and a waist diameter of 40 μ m, which defines a focal volume of ca. 5.8 nL. The generated 410 nm SH signal was collected and detected by a photomultiplier (R585; Hamamatsu), preamplified (SR 440; Stanford Research Systems) and processed through a correlated photon counting system (SR400; Stanford Research Systems).

All time-resolved SHS experiments began by first measuring the background SHS signal from the liquid jet circulating out of the reservoir containing 9 mL of the solution of the desired chemical composition (but without bacteria or liposomes). Once the background was established, after approximately 1 min (at the time denoted t = 0 s), 1 mL of the stock bacteria (or liposome) suspension was added into the reservoir. The working cell densities in the reservoir for each strain were as follows: E. coli $\sim 6 \times 10^8 \text{ mL}^{-1} \text{ (OD}_{600} \sim 0.8)$ and P. aeruginosa $\sim 5 \times 10^7 \text{ mL}^{-1}$ (OD₆₀₀ ~ 0.07). The final concentrations in the sample reservoir were 5.5 μM MG and 1% DMSO. All experiments were performed at pH 7.2 [buffer PBS(-)] and at room temperature. All measurements were repeated a minimum of N=3 times, and the average and uncertainty deduced from the multiple measurements were reported as data points.

It should be noted that, in its cationic form, MG exhibits an electronic resonance near 420 nm that facilitates resonantly enhanced SHS. Further, as indole is noncentrosymmetric, it is also SHG-active. However, because it lacks an electronic transition near 410 nm, it does not contribute significantly to the measured SHS signal. Likewise, all of the other molecules in the samples (e.g., DMSO) do not produce detectable SHS signal.

ASSOCIATED CONTENT

Supporting Information

The Supporting Information is available free of charge at https://pubs.acs.org/doi/10.1021/acsinfecdis.1c00618.

Kovacs assay for determining the nascent extracellular and intracellular concentrations of indole; a kinetic model of molecular uptake in Gram-negative bacteria; output fit parameters based upon analysis using our kinetic model of molecular uptake; UV–vis spectra indole, malachite green, and a mixture of the two; growth kinetic curves (OD₆₀₀) of *E. coli BW25113* in the presence of increasing concentrations of DMSO; and schematic of our kinetic model of molecular uptake in Gram-negative bacteria (PDF)

AUTHOR INFORMATION

Corresponding Author

Michael J. Wilhelm — Department of Chemistry, Temple University, Philadelphia, Pennsylvania 19122, United States; orcid.org/0000-0002-4634-9561;

Email: michael.wilhelm@alumni.upenn.edu

Authors

Tong Wu — Department of Chemistry, Temple University, Philadelphia, Pennsylvania 19122, United States

Yujie Li — Department of Chemistry, Temple University, Philadelphia, Pennsylvania 19122, United States

Jianqiang Ma — Department of Chemistry, Temple University, Philadelphia, Pennsylvania 19122, United States

Hai-Lung Dai — Department of Chemistry, Temple University, Philadelphia, Pennsylvania 19122, United States;

orcid.org/0000-0001-6925-8075

Complete contact information is available at: https://pubs.acs.org/10.1021/acsinfecdis.1c00618

Author Contributions

T.W., M.J.W., and H.-L.D. designed the study. T.W. and Y.L. conducted the experiments. T.W. analyzed the data. T.W., M.J.W., J.M., and H.-L.D. interpreted the results. T.W., M.J.W., and H.-L.D. wrote the manuscript

Notes

The authors declare no competing financial interest. The data that support the findings of this study are available from the corresponding author upon reasonable request.

ACKNOWLEDGMENTS

This work was supported by the National Science Foundation (CHE-1465096). The authors wish to thank Feng Gai (University of Pennsylvania, Department of Chemistry) for originally suggesting that we consider indole.

■ REFERENCES

- (1) Wang, D.; Ding, X.; Rather, P. N. Indole Can Act as an Extracellular Signal in *Escherichia coli*. *J. Bacteriol.* **2001**, 183, 4210–4216
- (2) Lee, J. H.; Lee, J. Indole as an Intercellular Signal in Microbial Communities. *FEMS Microbiol. Rev.* **2010**, *34*, 426–444.
- (3) Lee, J.; Jayaraman, A.; Wood, T. K. Indole Is an Inter-Species Biofilm Signal Mediated by SdiA. *BMC Microbiol.* **2007**, *7*, No. 42.
- (4) Bansal, T.; Alaniz, R. C.; Wood, T. K.; Jayaraman, A. The Bacterial Signal Indole Increases Epithelial-Cell Tight-Junction Resistance and Attenuates Indicators of Inflammation. *Proc. Natl. Acad. Sci. U.S.A.* **2010**, *107*, 228–233.
- (5) Hu, Y.; Kwan, B. W.; Osbourne, D. O.; Benedik, M. J.; Wood, T. K. Toxin YafQ Increases Persister Cell Formation by Reducing Indole Signalling. *Environ. Microbiol.* **2015**, *17*, 1275–1285.
- (6) Vega, N. M.; Allison, K. R.; Khalil, A. S.; Collins, J. J. Signaling-Mediated Bacterial Persister Formation. *Nat. Chem. Biol.* **2012**, *8*, 431–433.
- (7) Lee, J. H.; Kim, Y. G.; Gwon, G.; Wood, T. K.; Lee, J. Halogenated Indoles Eradicate Bacterial Persister Cells and Biofilms. *AMB Express* **2016**, *6*, No. 123.
- (8) Kwan, B. W.; Osbourne, D. O.; Hu, Y.; Benedik, M. J.; Wood, T. K. Phosphodiesterase DosP Increases Persistence by Reducing CAMP Which Reduces the Signal Indole. *Biotechnol. Bioeng.* **2015**, *112*, 588–600.
- (9) Kim, J.; Park, W. Indole: A Signaling Molecule or a Mere Metabolic Byproduct That Alters Bacterial Physiology at a High Concentration? *J. Microbiol.* **2015**, *53*, 421–428.

- (10) Lee, H. H.; Molla, M. N.; Cantor, C. R.; Collins, J. J. Bacterial Charity Work Leads to Population-Wide Resistance. *Nature* **2010**, 467. 82–85.
- (11) Chant, E. L.; Summers, D. K. Indole Signalling Contributes to the Stable Maintenance of *Escherichia coli* Multicopy Plasmids. *Mol. Microbiol.* **2007**, *63*, 35–43.
- (12) Lepri, S.; Buonerba, F.; Goracci, L.; Velilla, I.; Ruzziconi, R.; Schindler, B. D.; Seo, S. M.; Kaatz, G. W.; Cruciani, G. Indole Based Weapons to Fight Antibiotic Resistance: A Structure-Activity Relationship Study. *J. Med. Chem.* **2016**, *59*, 867–891.
- (13) Kawamura-Sato, K.; Shibayama, K.; Horii, T.; Iimuma, Y.; Arakawa, Y.; Ohta, M. Role of Multiple Efflux Pumps in *Escherichia coli* in Indole Expulsion. *FEMS Microbiol. Lett.* **1999**, *179*, 345–352.
- (14) Wei, G. Z.; Martin, K. A.; Xing, P. Y.; Agrawal, R.; Whiley, L.; Wood, T. K.; Hejndorf, S.; Ng, Y. Z.; Low, J. Z. Y.; Rossant, J.; Nechanitzky, R.; Holmes, E.; Nicholson, J. K.; Tan, E.-K.; Matthews, P. M.; Pettersson, S. Tryptophan-Metabolizing Gut Microbes Regulate Adult Neurogenesis via the Aryl Hydrocarbon Receptor. *Proc. Natl. Acad. Sci. U.S.A.* 2021, 118, No. e2021091118.
- (15) Jaglin, M.; Rhimi, M.; Philippe, C.; Pons, N.; Bruneau, A.; Goustard, B.; Daugé, V.; Maguin, E.; Naudon, L.; Rabot, S. Indole, a Signaling Molecule Produced by the Gut Microbiota, Negatively Impacts Emotional Behaviors in Rats. *Front. Neurosci.* **2018**, *12*, No. 216.
- (16) Kim, W. H.; Lillehoj, H. S.; Min, W. Indole Treatment Alleviates Intestinal Tissue Damage Induced by Chicken Coccidiosis through Activation of the Aryl Hydrocarbon Receptor. *Front. Immunol.* **2019**, *10*, No. 560.
- (17) Yu, J.; Luo, Y.; Zhu, Z.; Zhou, Y.; Sun, L.; Gao, J.; Sun, J.; Wang, G.; Yao, X.; Li, W. A Tryptophan Metabolite of the Skin Microbiota Attenuates Inflammation in Patients with Atopic Dermatitis through the Aryl Hydrocarbon Receptor. *J. Allergy Clin. Immunol.* **2019**, *143*, 2108–2119.e12.
- (18) Chyan, Y. J.; Poeggeler, B.; Omar, R. A.; Chain, D. G.; Frangione, B.; Ghiso, J.; Pappolla, M. A. Potent Neuroprotective Properties against the Alzheimer β -Amyloid by an Endogenous Melatonin-Related Indole Structure, Indole-3-Propionic Acid. *J. Biol. Chem.* **1999**, 274, 21937–21942.
- (19) Song, S.; Wood, T. K. Combatting Persister Cells With Substituted Indoles. *Front. Microbiol.* **2020**, *11*, No. 1565.
- (20) Kim, J. S.; Wood, T. K. Persistent Persister Misperceptions. Front. Microbiol. 2016, 7, No. 2134.
- (21) Lewis, K. Persister Cells, Dormancy and Infectious Disease. *Nat. Rev. Microbiol.* **2007**, *5*, 48–56.
- (22) Zarkan, A.; Liu, J.; Matuszewska, M.; Gaimster, H.; Summers, D. K. Local and Universal Action: The Paradoxes of Indole Signalling in Bacteria. *Trends Microbiol.* **2020**, *28*, 566–577.
- (23) Wang, Y.; Tian, T.; Zhang, J.; Jin, X.; Yue, H.; Zhang, X. H.; Du, L.; Bai, F. Indole Reverses Intrinsic Antibiotic Resistance by Activating a Novel Dual-Function Importer. *mBio* **2019**, *10*, No. e00676-19.
- (24) Masuda, Y.; Sakamoto, E.; Honjoh, K.; Miyamoto, T. Role of Toxin-Antitoxin-Regulated Persister Population and Indole in Bacterial Heat Tolerance. *Appl. Environ. Microbiol.* **2020**, *86*, No. e00935-20.
- (25) Zhang, W.; Yamasaki, R.; Song, S.; Wood, T. K. Interkingdom Signal Indole Inhibits *Pseudomonas aeruginosa* Persister Cell Waking. *J. Appl. Microbiol.* **2019**, *127*, 1768–1775.
- (26) Bean, R. C.; et al. Permeability of Lipid Bilayer Membranes to Organic Solutes. *J. Gen. Physiol.* **1968**, *52*, 495–508.
- (27) Chimerel, C.; Murray, A. J.; Oldewurtel, E. R.; Summers, D. K.; Keyser, U. F. The Effect of Bacterial Signal Indole on the Electrical Properties of Lipid Membranes. *ChemPhysChem* **2013**, *14*, 417–423.
- (28) Eisenbach, M.; Constantinou, C.; Aloni, H.; Shinitzky, M. Repellents for *Escherichia coli* Operate Neither by Changing Membrane Fluidity nor by Being Sensed by Periplasmic Receptors during Chemotaxis. *J. Bacteriol.* **1990**, *172*, 5218–5224.
- (29) Cama, J. Quantifying Passive Drug Transport Across Lipid Membranes. Ph.D. Thesis, University of Cambridge, 2015.

- (30) Wilhelm, M. J.; Dai, H. Molecule-Membrane Interactions in Biological Cells Studied with Second Harmonic Light Scattering. *Chem. Asian J.* **2020**, *15*, 198.
- (31) Wilhelm, M. J.; Sharifian Gh, M.; Dai, H. L. Influence of Molecular Structure on Passive Membrane Transport: A Case Study by Second Harmonic Light Scattering. *J. Chem. Phys.* **2019**, *150*, No. 104705.
- (32) Wilhelm, M. J.; Sharifian Gh, M.; Dai, H. L. Support Information Chemically Induced Changes to Membrane Permeability in Living Cells Probed with Nonlinear Light Scattering. *Biochemistry* **2015**, *54*, 4427–4430.
- (33) Eisenthal, K. B. Liquid Interfaces Probed by Second-Harmonic and Sum-Frequency Spectroscopy. *Chem. Rev.* **1996**, *96*, 1343–1360.
- (34) Roke, S.; Gonella, G. Nonlinear Light Scattering and Spectroscopy of Particles and Droplets in Liquids. *Annu. Rev. Phys. Chem.* **2012**, *63*, 353–378.
- (35) Gonella, G.; Dai, H. L. Second Harmonic Light Scattering from the Surface of Colloidal Objects: Theory and Applications. *Langmuir* **2014**, *30*, 2588–2599.
- (36) Wang, H.; Borguet, E.; Eisenthal, K. B. Polarity of Liquid Interfaces by Second Harmonic Generation Spectroscopy. *J. Phys. Chem. A* **1997**, *101*, 713–718.
- (37) Liu, Y.; Yan, E. C. Y.; Eisenthal, K. B. Effects of Bilayer Surface Charge Density on Molecular Adsorption and Transport across Liposome Bilayers. *Biophys. J.* **2001**, *80*, 1004–1012.
- (38) Liu, J.; Subir, M.; Nguyen, K.; Eisenthal, K. B. Second Harmonie Studies of Ions Crossing Liposome Membranes in Real Time. J. Phys. Chem. B 2008, 112, 15263–15266.
- (39) Hamal, P.; Nguyenhuu, H.; Subasinghege Don, V.; Kumal, R. R.; Kumar, R.; McCarley, R. L.; Haber, L. H. Molecular Adsorption and Transport at Liposome Surfaces Studied by Molecular Dynamics Simulations and Second Harmonic Generation Spectroscopy. *J. Phys. Chem. B* **2019**, *123*, 7722–7730.
- (40) Kumal, R. R.; Nguyenhuu, H.; Winter, J. E.; McCarley, R. L.; Haber, L. H. Impacts of Salt, Buffer, and Lipid Nature on Molecular Adsorption and Transport in Liposomes As Observed by Second Harmonic Generation. *J. Phys. Chem. C* **2017**, *121*, 15851–15860.
- (41) Hou, Y.; Chen, S. L.; Gan, W.; Ma, X.; Yuan, Q. Understanding the Dynamic Behavior of an Anticancer Drug, Doxorubicin, on a Lipid Membrane Using Multiple Spectroscopic Techniques. *J. Phys. Chem. B* **2019**, *123*, 3756–3762.
- (42) Okur, H. I.; Tarun, O. B.; Roke, S. Chemistry of Lipid Membranes from Models to Living Systems: A Perspective of Hydration, Surface Potential, Curvature, Confinement and Heterogeneity. J. Am. Chem. Soc. 2019, 141, 12168–12181.
- (43) Miller, L. N.; Brewer, W. T.; Williams, J. D.; Fozo, E. M.; Calhoun, T. R. Second Harmonic Generation Spectroscopy of Membrane Probe Dynamics in Gram-Positive Bacteria. *Biophys. J.* **2019**, *117*, 1419–1428.
- (44) Wilhelm, M. J.; Sharifian Gh, M.; Wu, T.; Li, Y.; Chang, C.-M.; Ma, J.; Dai, H.-L. Determination of Bacterial Surface Charge Density via Saturation of Adsorbed Ions. *Biophys. J.* **2021**, *120*, 2461–2470.
- (45) Zeng, J.; Eckenrode, H. M.; Dounce, S. M.; Dai, H. L. Time-Resolved Molecular Transport across Living Cell Membranes. *Biophys. J.* **2013**, *104*, 139–145.
- (46) Wilhelm, M. J.; Sheffield, J. B.; Gonella, G.; Wu, Y.; Spahr, C.; Zeng, J.; Xu, B.; Dai, H. L. Real-Time Molecular Uptake and Membrane-Specific Transport in Living Cells by Optical Microscopy and Nonlinear Light Scattering. *Chem. Phys. Lett.* **2014**, 605–606, 158–163.
- (47) Wilhelm, M. J.; Sheffield, J. B.; Sharifian Gh, M.; Wu, Y.; Spahr, C.; Gonella, G.; Xu, B.; Dai, H. L. Gram's Stain Does Not Cross the Bacterial Cytoplasmic Membrane. *ACS Chem. Biol.* **2015**, *10*, 1711–1717
- (48) Gayen, A.; Kumar, D.; Matheshwaran, S.; Chandra, M. Unveiling the Modulating Role of Extracellular PH in Permeation and Accumulation of Small Molecules in Subcellular Compartments of Gram-Negative *Escherichia coli* Using Nonlinear Spectroscopy. *Anal. Chem.* **2019**, *91*, 7662–7671.

ACS Infectious Diseases Article pubs.acs.org/journal/aidcbc

- (49) Sharifian Gh, M.; Wilhelm, M. J.; Dai, H. L. Label-Free Optical Method for Quantifying Molecular Transport Across Cellular Membranes in Vitro. J. Phys. Chem. Lett. 2016, 7, 3406-3411.
- (50) Gh, M. S.; Wilhelm, M. J.; Dai, H. L. Azithromycin-Induced Changes to Bacterial Membrane Properties Monitored in Vitro by Second-Harmonic Light Scattering. ACS Med. Chem. Lett. 2018, 9,
- (51) Forman, M. E.; Fletcher, M. H.; Jennings, M. C.; Duggan, S. M.; Minbiole, K. P. C.; Wuest, W. M. Structure-Resistance Relationships: Interrogating Antiseptic Resistance in Bacteria with Multicationic Quaternary Ammonium Dyes. ChemMedChem 2016, 11, 958-962.
- (52) Lee, J.; Attila, C.; Cirillo, S. L. G.; Cirillo, J. D.; Wood, T. K. Indole and 7-Hydroxyindole Diminish Pseudomonas aeruginosa Virulence. Microb. Biotechnol. 2009, 2, 75-90.
- (53) Chu, W.; Zere, T. R.; Weber, M. M.; Wood, T. K.; Whiteley, M.; Hidalgo-Romano, B.; Valenzuela, E.; McLean, R. J. C. Indole Production Promotes Escherichia coli Mixed-Culture Growth with Pseudomonas aeruginosa by Inhibiting Quorum Signaling. Appl. Environ. Microbiol. 2012, 78, 411-419.
- (54) Li, G.; Young, K. D. Indole Production by the Tryptophanase TnaA in Escherichia coli Is Determined by the Amount of Exogenous Tryptophan. Microbiology 2013, 159, 402-410.
- (55) Sharifian Gh, M.; Wilhelm, M. J.; Moore, M.; Dai, H. L. Spatially Resolved Membrane Transport in a Single Cell Imaged by Second Harmonic Light Scattering. Biochemistry 2019, 58, 1841-1844.
- (56) Yan, E. C. Y.; Eisenthal, K. B. Effect of Cholesterol on Molecular Transport of Organic Cations across Liposome Bilayers Probed by Second Harmonic Generation. Biophys. J. 2000, 79, 898-
- (57) Sarsero, J. P.; Wookey, P. J.; Gollnick, P.; Yanofsky, C.; Pittard, A. J. A New Family of Integral Membrane Proteins Involved in Transport of Aromatic Amino Acids in Escherichia coli. J. Bacteriol. 1991, 173, 3231-3234.
- (58) Sarsero, J. P.; Pittard, A. J. Membrane Topology Analysis of Escherichia coli K-12 Mtr Permease by Alkaline Phosphatase and β -Galactosidase Fusions. J. Bacteriol. 1995, 177, 297-306.
- (59) Alberts, B.; Johnson, A.; Lewis, J.; Raff, M.; Roberts, K.; Walter, P. Carrier Proteins and Active Membrane Transport. In Molecular Biology of the Cell; Garland Science: New York, 2002.
- (60) Vollmer, W.; Blanot, D.; De Pedro, M. A. Peptidoglycan Structure and Architecture. FEMS Microbiol. Rev. 2008, 32, 149-167.
- (61) Raval, N. P.; Shah, P. U.; Shah, N. K. Malachite Green "a Cationic Dye" and Its Removal from Aqueous Solution by Adsorption. Appl. Water Sci. 2017, 7, 3407-3445.
- (62) Tang, H.; Zhou, W.; Zhang, L. Adsorption Isotherms and Kinetics Studies of Malachite Green on Chitin Hydrogels. J. Hazard. Mater. 2012, 209-210, 218-225.
- (63) Kang, C.; Korter, T. M.; Pratt, D. W. Experimental Measurement of the Induced Dipole Moment of an Isolated Molecule in Its Ground and Electronically Excited States: Indole and Indole-H2O. J. Chem. Phys. 2005, 122, No. 174301.
- (64) Abou-Hatab, S.; Matsika, S. Theoretical Investigation of Positional Substitution and Solvent Effects on N-Cyanoindole Fluorescent Probes. J. Phys. Chem. B 2019, 123, 7424-7435.
- (65) Norman, K. E.; Nymeyer, H. Indole Localization in Lipid Membranes Revealed by Molecular Simulation. Biophys. J. 2006, 91, 2046-2054.
- (66) Gaede, H. C.; Yau, W. M.; Gawrisch, K. Electrostatic Contributions to Indole-Lipid Interactions. J. Phys. Chem. B 2005, 109, 13014-13023.
- (67) Epand, R. M.; Walker, C.; Epand, R. F.; Magarvey, N. A. Molecular Mechanisms of Membrane Targeting Antibiotics. Biochim. Biophys. Acta, Biomembr. 2016, 1858, 980-987.
- (68) Kohanski, M. A.; Dwyer, D. J.; Collins, J. J. How Antibiotics Kill Bacteria: From Targets to Networks. Nat. Rev. Microbiol. 2010, 8, 423-435.

- (69) Davis, B. D.; Chen, L.; Tai, P. C. Misread Protein Creates Membrane Channels: An Essential Step in the Bactericidal Action of Aminoglycosides. Proc. Natl. Acad. Sci. U.S.A. 1986, 83, 6164-6168.
- (70) Kaldalu, N.; Mei, R.; Lewis, K. Killing by Ampicillin and Ofloxacin Induces Overlapping Changes in Escherichia coli Transcription Profile. Antimicrob. Agents Chemother. 2004, 48, 890-896.
- (71) Miyake, Y.; Fujiwara, S.; Usui, T.; Suginaka, H. Simple Method for Measuring the Antibiotic Concentration Required to Kill Adherent Bacteria. Chemotherapy 1992, 38, 286-290.
- (72) Baba, T.; Ara, T.; Hasegawa, M.; Takai, Y.; Okumura, Y.; Baba, M.; Datsenko, K. A.; Tomita, M.; Wanner, B. L.; Mori, H. Construction of Escherichia coli K-12 in-Frame, Single-Gene Knockout Mutants: The Keio Collection. Mol. Syst. Biol. 2006, 2, No. 2006,0008.
- (73) Liu, J.; Summers, D. Indole at Low Concentration Helps Exponentially Growing Escherichia coli Survive at High Temperature. PLoS One 2017, 12, No. e0188853.
- (74) Gaimster, H.; Summers, D. Regulation of Indole Signalling during the Transition of E. coli from Exponential to Stationary Phase. PLoS One 2015, 10, No. e0136691.
- (75) Zhang, H. Thin-Film Hydration Followed by Extrusion Method for Liposome Preparation. In Liposomes; Humana Press: New York, NY, 2017; Vol. 1522, pp 17-22.
- (76) Mitchell, S. A. Indole Adsorption to a Lipid Monolayer Studied by Optical Second Harmonic Generation. J. Phys. Chem. B 2009, 113, 10693-10707.

□ Recommended by ACS

Morphological Characterization of Antibiotic Combinations

Marc A. Coram, Brian Y. Feng, et al.

DECEMBER 22 2021

ACS INFECTIOUS DISEASES

READ 2

Qualitative and Quantitative Changes to Escherichia coli during Treatment with Magainin 2 Observed in **Native Conditions by Atomic Force Microscopy**

Kanesha Overton, Catherine B. Volle, et al.

DECEMBER 26, 2019

LANGMUIR

READ **C**

S. boulardii Fails to Hold Its Cell Wall Integrity against Nonpathogenic E. coli: Are Probiotic Yeasts Losing the

Satyajit Lenka, Manabendra Chandra, et al.

MARCH 11, 2021

ACS INFECTIOUS DISEASES

READ C

Clinically Relevant Bacterial Outer Membrane Models for Antibiotic Screening Applications

Zeinab Mohamed, Susan Daniel, et al.

JULY 06, 2021

ACS INFECTIOUS DISEASES

READ 🗹

Get More Suggestions >